FUDMA Journal of Sciences (FJS)
ISSN online: 2616-1370
ISSN print: 2645 - 2944
Vol. 10 No. 24, December, 2026, pp 79 – 92
DOI: https://doi.org/10.33003/fjs-2026-1024-6321

In Silico Assessment of *Gongronema Latifolium* Fruit Metabolites as Potential Multi-Target Antidiabetic Leads using Network Pharmacology and Molecular Docking

***Victoria Temitope Makanjuola, Gideon Ampoma Gyebi and Chinenye Florence Ogah**

Department of Biochemistry, Faculty of Science and Technology, Bingham University, Karu, Nasarawa State, Nigeria.

*Corresponding authors' email: victoriatope214@gmail.com Phone: +234 8135107717

Received: 26 Oct. 2026
Accepted: 08 Nov. 2026
Published: 09 Nov. 2026

ABSTRACT

Background: Type 2 diabetes mellitus (T2DM) is a multifactorial disease for which single-target drugs are often inadequate. The fruit of Gongronema latifolium is used in traditional Nigerian medicine, but its metabolites and molecular targets are poorly described.

Methods: Metabolites previously identified from the fruit were screened against Lipinski's rule of five and, in SwissADME, for gastrointestinal absorption and drug-likeness. Their targets were predicted and intersected with T2DM-associated genes, a protein–protein interaction network was analysed to identify hub genes, and Gene Ontology and KEGG enrichment was performed. The retained metabolites were docked against two hub targets, AKT1 and GAPDH.

Results: Of 251 metabolites that satisfied Lipinski's rule of five, 241 were retained after SwissADME screening. A total of 1561 targets were identified for the G. latifolium fruit compounds and 6,392 genes were associated with type 2 diabetes mellitus, of which 1,028 overlapped and were taken forward as common targets. Network analysis identified 25 hub genes, led by GAPDH, AKT1, TP53, INS and TNF. The best docking score for AKT1 was −11.9 kcal/mol, with −9.4 kcal/mol being the score for the co-crystallised ligand; for GAPDH, it was −9.7 kcal/mol, while the co-crystallised ligand had a score of −7.0 kcal/mol. Twenty metabolites outscored both references, and C20 and C513 ranked highly for both targets.

Conclusion: Metabolites of G. latifolium fruit are predicted to engage several T2DM-relevant targets, notably insulin-signalling and inflammatory nodes, supporting the traditional use of the fruit and prioritising candidates for in vitro and in vivo validation.

Keywords: *Gongronema latifolium,* network pharmacology, molecular docking, type 2 diabetes mellitus, AKT1, GAPDH

INTRODUCTION

Diabetes mellitus is among the most pressing health problems of the twenty first century. In 2024, the International Diabetes Federation (IDF) estimated that there were 589 million adults aged from 20 to 79 years living with diabetes, which is projected to rise to 853 million by 2050, and that over 3.4 million people died of diabetes each year (Genitsaridi *et al.,* 2026). Over 90% of cases are type 2 diabetes mellitus (T2DM), which is a chronic metabolic disorder caused by insulin resistance and gradual onset of β-cell dysfunction results in chronic hyperglycaemia (Accili *et al.,* 2025). Chronic hyperglycaemia causes oxidative stress, chronic inflammation and microvascular and macrovascular complications over time, such as cardiovascular disease, nephropathy, retinopathy and neuropathy (Młynarska *et al.,* 2025).

One of the major characteristics of T2DM and a treatment target is postprandial hyperglycaemia. The dietary carbohydrates are hydrolyzed by the enzyme α-amylase and α-glucosidase to glucose which can be absorbed, and so inhibiting these enzymes helps to reduce the release of glucose after meals, which diminishes postprandial spikes in blood sugar. Hyperglycaemia also raises aldose reductase activity, leading to the diversion of glucose into the path of diabetic complications, the polyol pathway. These processes work synergistically and modulating one target is not sufficient to get a complete picture about anti-diabetic activity. For this reason, carbohydrate digesting enzymes are of interest for searching for new anti-diabetic leads, as are the polyol-pathway enzymes and the broader network of human proteins associated with these enzymes and their involvement in disease. In addition to these enzymes, insulin signalling through the PI3K–AKT pathway is diminished in insulin resistance, which stimulates glucose uptake and glycogen formation, and represents a second therapeutic target (Huang *et al.,* 2018). Hyperglycaemia-induced glycolytic stress through glyceraldehyde-3-phosphate dehydrogenase (GAPDH) is another potential point of intervention for diabetic complications (Brownlee, 2005). Existing medicines tend to have side effects and become ineffective over time (Mahmoud *et al.,* 2024), and the majority of them have been developed according to a 'one drug, one target' approach that is not appropriate for a multifactorial disease (Panossian, 2025). Medicinal plants are therefore of growing interest because phytochemicals of medicinal plants can act on several targets simultaneously and they are widely available and relatively inexpensive (Mahmoud *et al.,* 2024). They do not replace conventional drugs, but they can still serve as an excellent source for drug leads if their mechanisms can be properly deciphered (Mahmoud *et al.,* 2024).

Gongronema latifolium Benth. (Apocynaceae), known as "utazi" in Igbo, is a climbing shrub of the tropical rainforest of West and Central Africa. It is eaten as a leafy vegetable (Gyebi *et al.,* 2024) and used in traditional medicine for diabetes, malaria, hepatitis and stomach disorders (Amrelia, 2022). It has been reported that flavonoids, saponins,

alkaloids and steroidal compounds are present in the plant, which has hypoglycaemic, hypolipidaemic, antioxidant and antimicrobial activity (Amrelia, 2022). Pregnane-type compounds from *G. latifolium* have been shown to interact with α-amylase, combining experimental activity with molecular modelling to explain the likely mechanism (Ogunyemi *et al.,* 2022), and iloneoside has been reported from the leaves (Gyebi *et al.,* 2024). More recent work used UHPLC–Orbitrap mass spectrometry to identify phenolic compounds, flavonoids such as kaempferol, coumarins such as scopolin and oxidised fatty acids in the leaf extract, and combined this with molecular docking (Beshel *et al.,* 2025). Most of this literature, however, concerns the leaves. A comparison of aqueous extracts reported higher tannin, total phenolic and flavonoid contents in the fruit than in the leaf (Okochi *et al.,* 2024), which suggests that the fruit is a source of biologically relevant metabolites. However, the individual components of the fruit and the molecular pathways by which they may affect glucose regulation are not well characterized. Complex multicomponent extracts are difficult to study with conventional experiments alone. Network pharmacology is a systems-level approach, which takes a "network-target, multiple-component" therapeutics approach instead of the traditional "one target, one drug" paradigm (Panossian, 2025). It maps how phytochemicals, their predicted protein targets and disease-associated genes and pathways are connected, which helps identify hub targets and key signalling pathways. In practice, predicted targets of the compounds are intersected with genes known to be associated with the disease, and topological analysis of the resulting protein–protein interaction network highlights highly connected proteins that may act as hub targets and the pathways in which they take part. Molecular docking can complement this by predicting the binding pose and affinity of a ligand to a target within the binding site and is widely used for prioritising candidates and investigating mechanisms of action (Paggi *et al.,* 2024). Although docking has its limitations (Paggi *et al.,* 2024), promising complexes are often taken forward for further testing, such as molecular dynamics simulation and binding free-energy calculations, to check that the predicted interactions are maintained over time. The prediction of drug-likeness and ADMET properties is another filter, as it eliminates candidates that are likely to have poor pharmacokinetics or toxicity issues early on in the costly experimental testing phase. Together, these approaches make an efficient pipeline for generating testable hypotheses before *in vitro* and *in vivo* work, and they have recently been used to explore the antidiabetic potential of *Salvia officinalis* (Ononamadu & Seidel, 2024), *Melissa officinalis* (Ononamadu *et al.,* 2025) and several Indonesian ethnomedicinal plants (Zubair *et al.,* 2025).

To the best of our knowledge, no study has combined network pharmacology and molecular docking to examine the multi-target antidiabetic potential of the secondary metabolites of *G. latifolium* fruit. Addressing this gap can help elucidate the molecular basis of the traditional use of the fruit, reveal the most probable metabolites responsible for the antidiabetic activity, and identify lead compounds for development. Because plant extracts contain many metabolites, a step-wise computational approach that prioritises candidates for experimental testing is practical. This study thus used an integrated computational pathway for the metabolites already found in the fruit of *G. latifolium*. Specifically, we aimed to (i) screen the metabolites for drug-likeness and predict their pharmacokinetic properties, (ii) use network pharmacology to identify the human targets, hub genes and pathways through which the metabolites may exert antidiabetic effects, and (iii) dock the retained metabolites against the prioritised hub targets, AKT1 and GAPDH, to identify the most promising binders. The study thus seeks to offer a molecular basis for the traditional use of the fruit in diabetes control and a prioritised list of potential metabolites and targets for further experimentation.

MATERIALS AND METHODS

Compound Library and Screening

The compounds used in this study were 251 metabolites previously identified from the fruit of *Gongronema latifolium* (reported separately and still in process) that satisfied Lipinski's rule of five (Lipinski *et al.,* 2001). These were further screened in SwissADME (Daina *et al.,* 2017) for high predicted gastrointestinal absorption and drug-likeness, and 241 metabolites were retained for target prediction and docking. SMILES were obtained from PubChem (Kim *et al.,* 2025).

Network Pharmacology

Target Prediction

SMILES were submitted to SwissTargetPrediction for Homo sapiens (Daina *et al.,* 2019), keeping targets with a probability of at least 0.1. PharmMapper (Wang *et al.,* 2017) added targets to improve coverage.

Diabetes Targets and the Overlap

Genes linked to diabetes mellitus and type 2 diabetes were retrieved from DisGeNET (Piñero *et al.,* 2020), MalaCards (Rappaport *et al.,* 2017) and OMIM (Amberger *et al.,* 2019) using diabetes-related keywords. After removing duplicates, the compound targets were intersected with the disease genes to obtain the common targets, and the overlap was shown as a Venn diagram. The workflow was adapted from Ojo *et al.* (2025, 2026).

Networks and Hub Targets

A compound–target network was built in Cytoscape 3.9.1 (Shannon *et al.,* 2003). Common targets were submitted to STRING (Szklarczyk *et al.,* 2025; Homo sapiens, high-confidence interaction score of ≥ 0.700) to create a protein–protein interaction network and disconnected nodes were removed. Nodes were ranked by degree, betweenness centrality and closeness centrality, and the top 20 hub targets were identified with CytoHubba (Chin *et al.,* 2014).

Enrichment Analysis

GO terms (biological process, molecular function, cellular component) and KEGG pathways were enriched for the 25 hub genes in ShinyGO (Ge *et al.,* 2020), with an FDR < 0.05.

Molecular Docking

Molecular docking was performed against two hub targets identified from the protein–protein interaction (PPI) analysis, AKT1 (PDB ID: 4EKL) and GAPDH (PDB ID: 6M61), to predict the binding affinities and interaction modes of the retained metabolites. The workflow used for docking was based on the well established structure based virtual screening (SBVS) methods employed in computational drug discovery and network pharmacology studies.

Ligand Preparation

The two-dimensional structures of the 241 retained metabolites were retrieved from PubChem (Kim et al., 2025) in Structure Data File (SDF) format and imported into PyRx (Dallakyan & Olson, 2015). The structures were converted into three-dimensional conformations and energy-minimised

using Open Babel (O'Boyle *et al.,* 2011) with the Universal Force Field (UFF; Rappé *et al.,* 1992) and the conjugate gradient algorithm for 200 steps. The minimized ligands were then converted to PDBQT format and the rotatable bonds were identified for docking, while the Gasteiger partial charges were assigned.

Protein Preparation

The crystallographic structures of AKT1 and GAPDH were retrieved from the Research Collaboratory for Structural Bioinformatics Protein Data Bank (RCSB PDB; Berman *et al.,* 2000). Water molecules, co-solvents and non-essential heteroatoms were removed from the protein structures. The co-crystallised ligand of each protein was extracted and saved separately for redocking validation and reference purposes. Polar hydrogen atoms and Kollman partial charges were added, after which the prepared protein structures were converted into PDBQT format using the appropriate preparation tools in PyRx.

Grid Generation and Docking

The docking grid for each target was centred on the binding site associated with the co-crystallised ligand. For AKT1 (PDB ID: 4EKL), the grid dimensions set to 30.4497 × 29.5329 × 27.2303 Å. For GAPDH (PDB ID: 6M61), the grid centre was set to x = −15.666, y = 6.041 and z = −22.870. The docking was carried out by AutoDock Vina version 1.1.2 (Trott & Olson, 2010), using PyRx, with an exhaustiveness value of 8. The number of poses generated for each ligand was 9. The pose with the most negative predicted binding affinity (kcal/mol) was selected as the best-scoring pose. The co-crystallised ligand of each target was also docked under the same conditions to provide a reference for comparing the predicted binding affinities and evaluating the docking protocol.

Interaction Analysis

The best-scoring protein–ligand complexes were visualised using BIOVIA Discovery Studio Visualizer. The interactions between the retained metabolites and the binding-site residues of AKT1 and GAPDH were examined to identify hydrogen bonds, hydrophobic contacts, π–π stacking and other relevant non-covalent interactions. These interaction profiles were used to characterise the predicted binding modes and identify key amino acid residues potentially contributing to ligand binding.

RESULTS AND DISCUSSION

The study workflow has been summarized in Figure 1

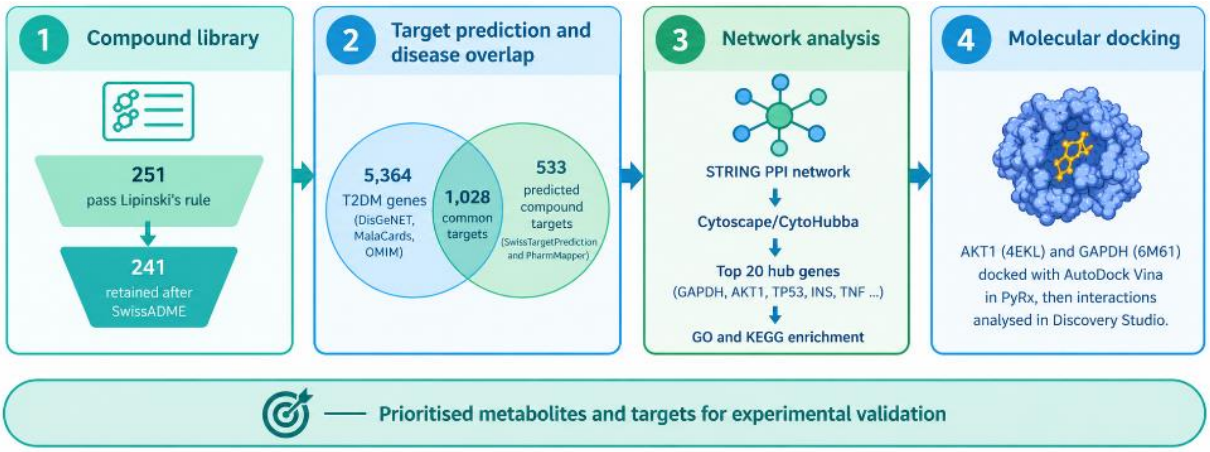


Figure 1: Workflow diagram. Metabolites previously identified from G. latifolium fruit were screened for drug-likeness and gastrointestinal absorption, and their targets were predicted using SwissTargetPrediction and PharmMapper. The predicted targets were intersected with T2DM-associated genes retrieved from DisGeNET, MalaCards and OMIM. Network pharmacology analyses, including compound–target network construction, protein–protein interaction analysis, hub gene identification, and Gene Ontology and KEGG pathway enrichment, were performed to investigate potential antidiabetic mechanisms. The selected metabolites were docked with AKT1 and GAPDH and the binding affinities and protein-ligand interactions were studied in order to identify potential phytochemicals and molecular targets for future experimental investigation.

Network Pharmacology

Network pharmacology was conducted, to identify the potential molecular targets of the secondary metabolites from *G. latifolium* fruits that could be shared with the genes associated with type 2 diabetes (T2D). The scaffolds that resulted from the overlapping targets were then analyzed for protein–protein interactions, hub gene identification, Gene Ontology enrichment and KEGG pathway analysis.

The Venn diagram (figure 2) shows the relationship between the set of genes associated with T2D and the set of predicted *G. latifolium* fruit compound protein targets. In total, 6,392 diabetes genes and 1,561 compound targets with 5,364 and 533 as the unique parts. 1,028 targets were common to both datasets, were associated with diabetes but not with compounds, and 533 were associated with compounds but not with diabetes.

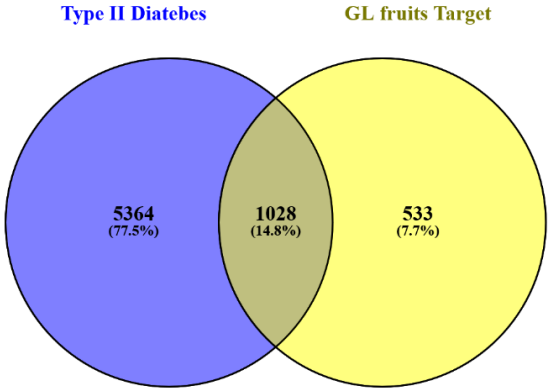


Figure 2: Venn diagram showing the overlap between type II diabetes-associated genes and predicted target proteins of *G. latifolium* fruit compounds

STRING PPI network shows PPIs among the common protein targets obtained from the overlap analysis (figure S1). Each node corresponds to a target protein itself, and the edges between nodes represent the predicted protein–protein associations in the network. The network is made up of a large number of interconnected nodes, and the spread of the connections gives the basis for the next step of discovering the highly connected hub targets.

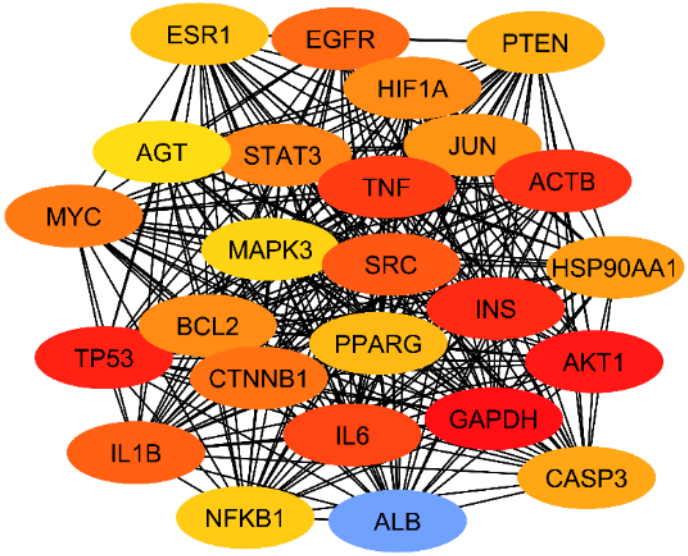


Figure 3: The top 25 hub genes were identified in the PPI network and are shown as the nodes in the Cytoscape network.

The twenty-five highest-ranked hub genes from the Cytoscape PPI analysis (Figure 3) based on the reported degree, closeness and betweenness measures are shown in Table 1. Making the following; GAPDH, AKT1, TP53, INS, ACTB, TNF and IL6were the highest-degree nodes in the network.

Table 1: Top 25 Hub Genes Identified from the Cytoscape PPI Network

Rank	Gene	Closeness	Betweenness	Degree
1	GAPDH	746.1667	49686.45	458
2	AKT1	741.1667	37469.97	447
3	TP53	735.4167	44436.25	438
4	INS	720.3333	46844.79	407
5	ACTB	719.75	24459.17	406
6	TNF	714.3333	26661.78	396
7	IL6	708.3333	24303.2	384
8	ALB	694.75	13327.06	359
9	SRC	689.5833	35822.43	351
10	IL1B	686.5	19133.48	341
11	EGFR	681.1667	19818.81	331
12	CTNNB1	678.75	18032.39	327
13	MYC	677.75	15562.04	326

Rank	Gene	Closeness	Betweenness	Degree
14	STAT3	674.25	9667.516	319
15	HIF1A	665.4167	9543.648	301
16	BCL2	665.4167	10778.04	300
17	JUN	662	9677.722	296
18	HSP90AA1	659.0833	13466.73	290
19	CASP3	656.5833	28442.03	285
20	PTEN	656.4167	8337.592	285
21	ESR1	653.3333	14589.47	279
22	PPARG	654.5833	14119.86	277
23	NFKB1	649.25	5580.092	270
24	MAPK3	649	9302.259	270
25	AGT	646.8333	25541.13	268

Abbreviations: GAPDH, glyceraldehyde-3-phosphate dehydrogenase; AKT1, AKT serine/threonine kinase 1; TP53, tumour protein p53; INS, insulin; ACTB, actin beta; TNF, tumour necrosis factor; IL6, interleukin 6; ALB, albumin; SRC, SRC proto-oncogene; IL1B, interleukin 1 beta; EGFR, epidermal growth factor receptor; CTNNB1, catenin beta 1; MYC, MYC proto-oncogene; STAT3, signal transducer and activator of transcription 3; HIF1A, hypoxia-inducible factor 1 alpha; BCL2, B-cell lymphoma 2; JUN, Jun proto-oncogene; HSP90AA1, heat shock protein 90 alpha family class A member 1; CASP3, caspase 3; PTEN, phosphatase and tensin homolog; ESR1, oestrogen receptor 1; PPARG, peroxisome proliferator-activated receptor gamma; NFKB1, nuclear factor kappa B subunit 1; MAPK3, mitogen-activated protein kinase 3; AGT, angiotensinogen.

A number of high-ranked nodes are highly connected housekeeping or abundant proteins (e.g. GAPDH, ACTB and ALB) and may not be disease-specific but rather linked to network topology. Therefore, AKT1 and GAPDH were chosen for docking because AKT1 is a central node of insulin signalling and glucose uptake and GAPDH is a key glycolytic enzyme whose dysregulation has been linked to diabetic complications.

The Gene Ontology biological-process enrichment plot (figure 4a) shows the enriched terms of the biological processes associated with the 25 hub genes. Enriched terms are positive regulation of DNA-templated transcription initiation, adherens junction organization, positive regulation of cyclin-dependent protein serine/threonine kinase activity, negative regulation of telomerase activity, negative regulation of post-transcriptional gene silencing, hyaluronan biosynthetic process, adherens junction assembly, RNA polymerase II preinitiation complex assembly, regulation of calcidiol 1-monooxygenase activity, T-helper 17 cell lineage commitment, aminoglycan biosynthetic process, glycosaminoglycan biosynthetic process, intestinal epithelial cell differentiation and development, and transcription preinitiation complex assembly. The x-axis shows the fold enrichment; the size of each point corresponds to the number of genes that are associated with the corresponding biological-process term. The colour scale represents −log10(FDR).

The cellular-component enrichment plot (Figure 4b) represents the cellular components related to the top 25 hub genes. The terms for cellular components are enriched with RNA polymerase II transcription regulator complex, transcription regulator complex, chromatin, euchromatin, transcription repressor complex, nucleoplasm, chromosome, nuclear lumen, RNA polymerase II transcription repressor complex, nuclear protein-containing complex and dendrite terminus and blood microparticle. The x-axis represents fold enrichment, and the size of the points reflects the number of genes contributing to the term, and the colour scale reflects the −log10(FDR) value.

The molecular-function enrichment plot (Figure 4c) displays the molecular functions of the top 25 hub genes. The enriched terms are: nuclear estrogen receptor binding, phosphatase binding, DNA-binding transcription repressor activity, RNA polymerase II-specific DNA-binding transcription activator and repressor activities, protein phosphatase binding, disordered domain-specific binding, nuclear receptor binding, E-box binding, general transcription initiation factor binding, ATPase binding, SMAD binding, mRNA binding, RNA polymerase II general transcription initiation factor binding, phospholipase activator activity, lipase activator activity, hormone activity, protein phosphatase 2A binding, and R-SMAD binding. The x axis shows fold enrichment, and the size of the points is a proxy for the number of genes that were found to be linked to each molecular-function term; the colour of the points corresponds to the −log10(FDR).

The KEGG pathway maps are graphical representations of the inflammatory bowel disease (Figure S2a) and type 1 diabetes mellitus pathways (Figure S2b), with the identified targets mapped onto their respective pathway components. The highlighted targets show the positions of the identified targets within the molecular components of these pathways, illustrating their potential involvement in the biological processes associated with inflammatory bowel disease and type 1 diabetes mellitus.

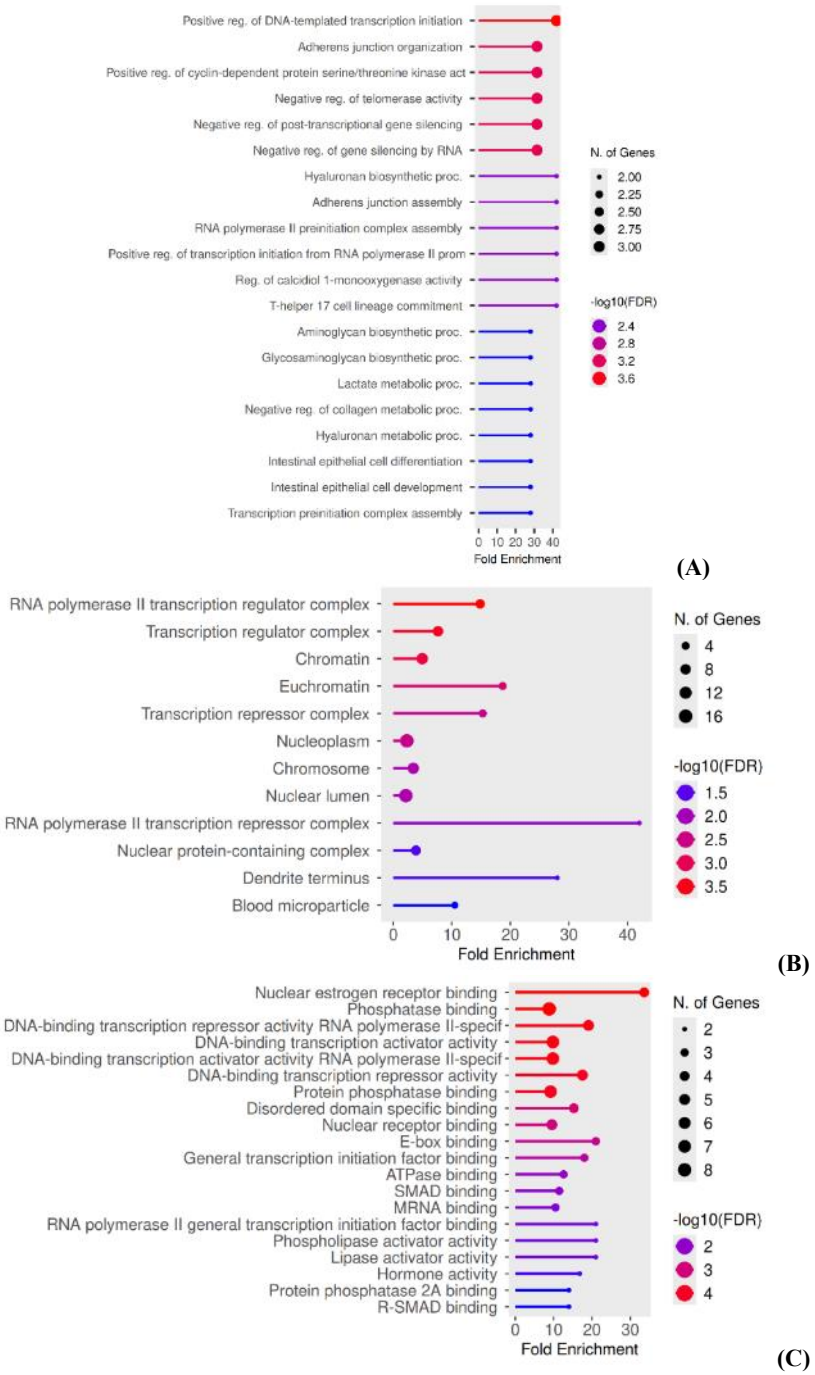


Figure 4: Gene Ontology enrichment analysis of (a) biological processes (b) cellular components (c) molecular function associated with the top 20 hub genes

Molecular Docking

Table 2: Top-scoring *G. Latifolium* Fruit Metabolites from Docking

Code	Compound Name	Class	Formula	Docking score (6M61) (kcal/mol)	Docking score (4EKL) (kcal/mol)
C20	1,3,4-trihydroxy-5-{[3-(4-hydroxyphenyl)prop-2-enoyl]oxy}cyclohexane-1-carboxylic acid	p-Coumaroylquinic acid derivative	$C_{16}H_{18}O_8$	-9.4	-11.0
C25	3-methyl-N-[4-[(3-phenylmethoxybenzoyl)amino]phenyl]benzamide	Synthetic-looking aromatic amide	$C_{28}H_{24}N_2O_3$	-9.4	-10.4
C34	1alpha,3alpha-Dihydroxy-4alpha-(4-hydroxycinnamoyloxy)-5beta-(3-methoxy-4-	Dicinnamoylquinic acid derivative	$C_{26}H_{26}O_{11}$	-8.1	-10.4

Code	Compound Name	Class	Formula	Docking score (6M61) (kcal/mol)	Docking score (4EKL) (kcal/mol)
	hydroxycinnamoyloxy)cyclohexane-1-carboxylic acid				
C151	(7R)-7-[(2-Amino-4-thiazolyl)(methoxyimino)acetylamino]-3-[4-(2-hydroxyethyl)pyridinium-1-ylmethyl]cepham-3-ene-4-carboxylic acid	Cephalosporin-type antibiotic	$C_{21}H_{22}N_6O_6S_2$	-8.7	-11.4
C296	Korglykon	Cardenolide/steroidal glycoside (Korglykon)	$C_{29}H_{42}O_{10}$	-7.8	-10.5
C513	Bis(3-butoxypropyl) but-2-enedioate	Dicarboxylic acid ester (aliphatic ester)	$C_{18}H_{32}O_6$	-9.3	-11.9
C1382	(5S,6S,7E,9E,11Z,13E,15S)-5,6,15-trihydroxyhenicosa-7,9,11,13-tetraenoic acid	Oxylipin / hydroxylated polyunsaturated fatty acid	$C_{21}H_{34}O_5$	-9.2	-6.0
C1403	1-[11-(1-Carboxycyclopropyl)-6-hydroxyundecyl]cyclopropane-1-carboxylic acid	Hydroxylated fatty acid derivative (cyclopropane-containing dicarboxylic acid)	$C_{19}H_{32}O_5$	-9.7	-6.1
C427	2-amino-3-[S-[(2R)-2-amino-2-carboxyethyl]-N-hydroxysulfinimidoyl]sulfanylpropanoic acid	Sulfur-containing amino acid derivative	$C_6H_{13}N_3O_5S_2$	-9.2	-10.6
C928	{1-acetyl-9a,11a-dimethyl-5-[(3,4,5-trihydroxy-6-methyloxan-2-yl)oxy]-1H,2H,3H,3aH,3bH,4H,5H,5aH,6H,7H,8H,9H,9aH,9bH,11aH-cyclopenta[a]phenanthren-7-yl}oxidanesulfonic acid	Steroidal glycoside/sulfonic acid derivative	$C_{27}H_{42}O_{10}S$	-8.1	-10.9

Table 3: Docking Scores (Binding Affinity, Kcal/mol) of selected Metabolites against AKT1 and GAPDH

Ligand	AKT1 (4EKL)	GAPDH (6M61)
Reference (co-crystallised/native ligand)	-9.4	-7.0
C20	-11.0	-9.4
C25	-10.4	-9.4
C34	-10.4	-8.1
C151	-11.4	-8.7
C296	-10.5	-7.8
C513	-11.9	-9.3
C928	-10.9	-8.1
C427	-10.6	-9.2
C1382	-6.0	-9.2
C1403	-6.1	-9.7

The retained metabolites were docked against AKT1 and GAPDH; the identities of the top-scoring metabolites are listed in Table 2, and their docking scores are given in Table 3. The binding affinities of AKT1 ranged from -11.9 to -4.7 kcal/mol and GAPDH from -9.7 to -3.9 kcal/mol. Twenty metabolites scored better than both reference ligands. The AKT1 co-crystallised ligand scored −9.4 kcal/mol, and C513 (−11.9), C151 (−11.4), C20 (−11.0), C928 (−10.9), C427 (−10.6) and C296 (−10.5) all scored better. For GAPDH, the reference scored −7.0 kcal/mol, and C1403 (−9.7), C28 (−9.4), C25 (−9.4) and C513 (−9.3) scored better. C20 and C513 were among the highest scoring compounds for both targets, indicating a dual-target potential. The binding poses and interactions of selected metabolites are shown in Figure 5 (AKT1) and Figure 6 (GAPDH) and summarised in Table 4

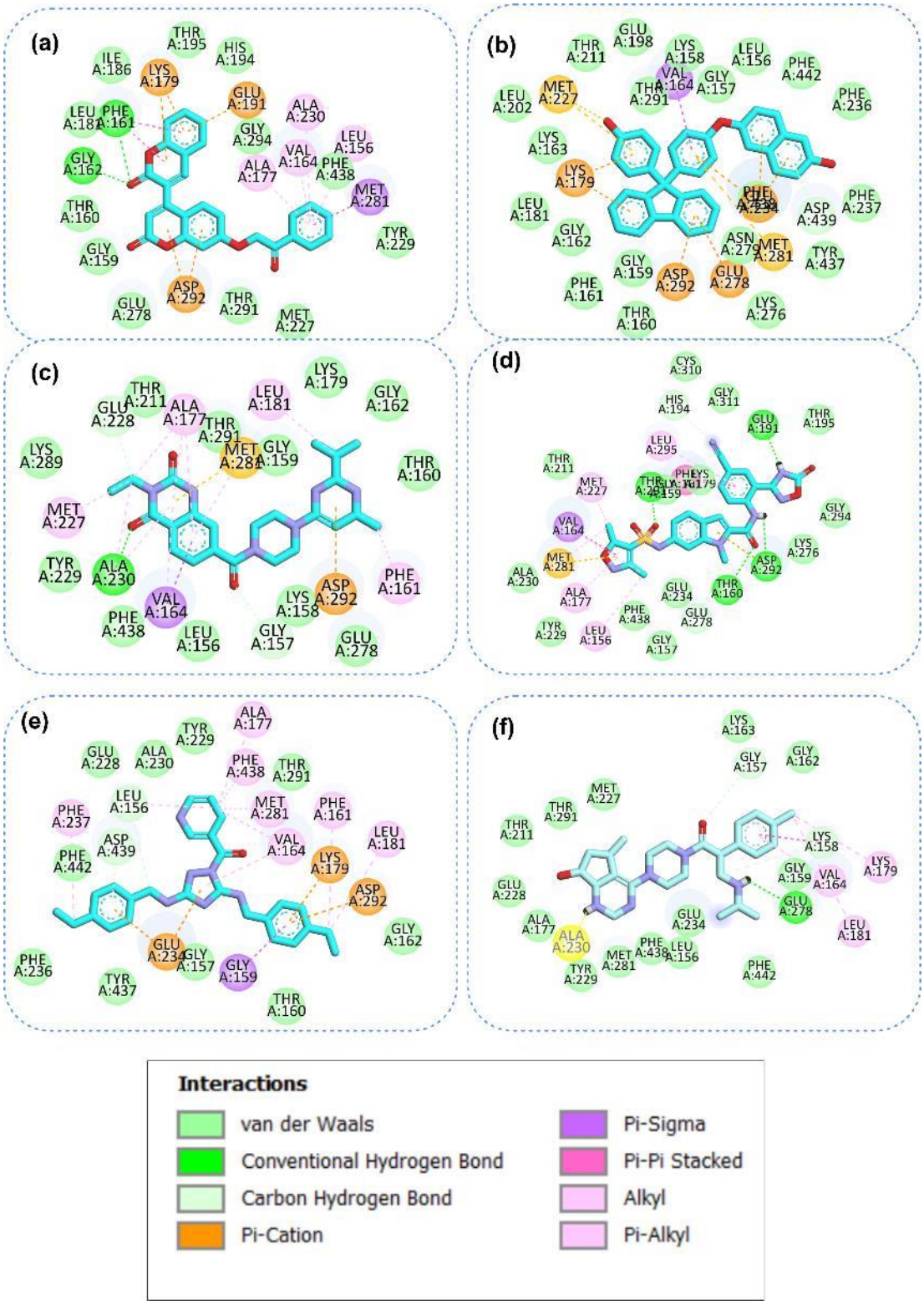


Figure 5: Amino acid interactive plots of top-five-secondary metabolites from *G. latifolium* fruits, identified from the docking analysis against AKT1: (a) C20; (b) C25; (c) C34; (d) C151; (e) C296; and (f) co-crystallised ligand

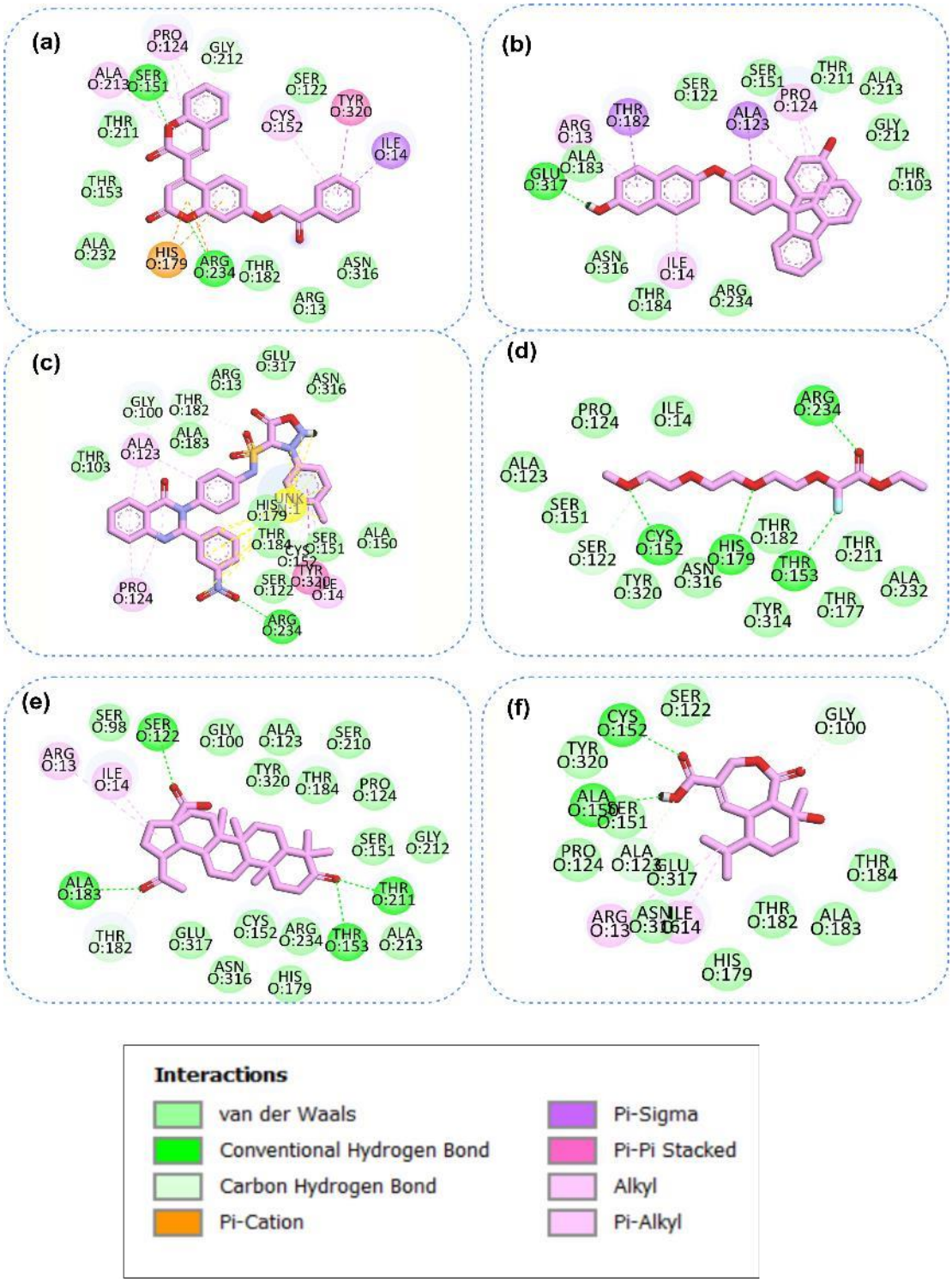


Figure 6: Amino acid interactive plots of top-five-secondary metabolites from *G. latifolium* fruits, identified from the docking analysis against Glyceraldehyde-3-phosphate dehydrogenase (GAPDH): (a) C20; (b) C25; (c) C513; (d) C531; (e) C1382; and (f) reference ligand (heptelidic acid)

Protein-Ligand Interactions

Table 4: Amino Acid Interactions of Secondary Metabolites from *G. Latifolium* Fruits

Target (PDB ID)	Compound	Hydrogen bonds	Hydrophobic interactions	Others
AKT1 (4EKL)	Reference (Ipatasertib)	PHE 161, GLY 162	LEU 156, VAL 164, ALA 177, LEU 181, ILE 186, MET 227, TYR 229, ALA 230, MET 281, PHE 438	HIS 14, GLY 159, THR 160, LYS 179, GLU 191, THR 195, GLU 278, THR 291, ASP 292, GLY 294
	C20	–	LEU 156, PHE 161, VAL 164, LEU 181, LEU 202, MET 227, PHE 236, PHE 237, MET 281	GLY 157, LYS 158, GLY 159, THR 160, GLY 162, LYS 163, LYS 179, GLU 198, THR 211, LYS 276, GLU 278, ASN 279, THR 291, ASP 292, ASP 437
	C25	ALA 230	LEU 156, PHE 161, VAL 164, ALA 177, LEU 181, MET 227, TYR 229, MET 281, PHE 438	GLY 157, LYS 158, GLY 159, THR 160, GLY 162, LYS 179, THR 211, GLU 228, GLU 278, LYS 289, THR 291, ASP 292
	C34	THR 160, GLU 191, THR 291, ASP 292	LEU 156, PHE 161, VAL 164, ALA 177, MET 227, TYR 229, ALA 230, MET 281, LEU 295, CYS 310, PHE 438	GLY 157, GLY 159, LYS 179, HIS 194, THR 195, THR 211, GLU 234, LYS 276, GLU 278, GLY 294, GLY 311
	C151	–	LEU 156, VAL 164, ALA 177, LEU 181, TYR 229, ALA 230, PHE 236, PHE 237, MET 281, TYR 437, PHE 438, PHE 442	GLY 157, GLY 159, THR 160, GLY 162, LYS 179, GLU 228, GLU 234, THR 291, ASP 292, ASP 439
	C296	GLU 278	LEU 156, VAL 164, ALA 177, LEU 181, MET 227, TYR 229, ALA 230, MET 281, PHE 438, PHE 442	GLY 157, LYS 158, GLY 159, GLY 162, LYS 163, LYS 179, THR 211, GLU 228, GLU 234, THR 291
GAPDH (6M61)	Reference (heptelidic acid)	SER 151, ARG 234	ILE 14, PRO 124, CYS 152, ALA 213, ALA 232, TYR 320	ARG 13, SER 122, THR 153, HIS 179, THR 182, THR 211, GLY 212, ASN 316
	C20	GLU 317	ILE 14, ALA 123, PRO 124, ALA 183, ALA 213	ARG 13, THR 103, SER 122, SER 151, THR 182, THR 184, THR 211, GLY 212, ARG 234, ASN 316
	C25	ARG 234	ILE 14, ALA 123, PRO 124, ALA 150, CYS 152, ALA 183, TYR 320	ARG 13, GLY 100, THR 103, SER 122, SER 151, HIS 179, THR 182, THR 184, ASN 316, GLU 317
	C513	CYS 152, THR 153, HIS 179, ARG 234	ILE 14, ALA 123, PRO 124, ALA 232, TYR 314, TYR 320	SER 122, SER 151, THR 177, THR 182, THR 211, ASN 316
	C1382	ALA 150, CYS 152	ILE 14, ALA 123, PRO 124, ALA 183, TYR 320	ARG 13, GLY 100, SER 122, SER 151, HIS 179, THR 182, THR 184, ASN 316, GLU 317

All five metabolites contacted LYS179, VAL164 and LEU156 of AKT1, as did the reference. C31 hydrogen-bonded with the hinge residue ALA230. For GAPDH, C513 and C1382 hydrogen-bonded with the catalytic CYS152, and C25, C513 and C1382 also contacted HIS179, as did the reference.

Discussion

This study integrated network pharmacology and molecular docking to explore how metabolites identified from the fruit of *Gongronema latifolium* may influence type 2 diabetes mellitus (T2DM) at the molecular level. Most earlier work on this plant has concentrated on the leaves (Beshel *et al.,* 2025; Ogunyemi *et al.,* 2022), and to our knowledge this is the first systems-level prediction of the targets of the fruit metabolites. Such a multi-factorial disease as T2DM is good for attracting medicinal plants because it is possible to act on several targets at once, which is what the workflow presented here does, which goes from the predicted targets of 241 drug-like metabolites to the disease network they perturb, to the hub proteins that organise that network, and finally to the binding of the metabolites to two of these hubs.

The predicted targets of the metabolites retained were intersected with 6,392 T2DM associated genes, which is typical of a multi-targeted plant-derived chemical library. Topological analysis of the resulting protein–protein interaction network identified 20 hub genes: GAPDH, AKT1, TP53, INS, ACTB, TNF, IL6, ALB, SRC, IL1B, EGFR, CTNNB1, MYC, STAT3, HIF1A, BCL2, JUN, HSP90AA1, CASP3 and PTEN. Some of these, such as AKT1, TNF, IL6, IL1B, STAT3, and INS, are situated at insulin signalling/low-grade inflammation crossroads. Chronic tissue inflammation is a key feature of obesity and T2DM, and it is seen in adipose tissue, liver, muscle and pancreatic islets, where it contributes to insulin resistance and β-cell dysfunction (Donath & Shoelson, 2011; Rohm *et al.,* 2022). The presence of these genes among the hubs is biologically coherent because they have roles in interfering with insulin signalling in target tissues (TNF-α and IL-6), impairing β-cell function (IL-1β) and transducing IL-6-family signals (STAT3). A similar set of hubs (TNF, TP53, AKT1 and STAT3) was reported for an antidiabetic herbal formulation (Ojo *et al.,* 2025), which suggests that the inflammation–insulin-signalling axis is a

recurring feature of multi-target antidiabetic interventions. These highly connected nodes (e.g. GAPDH, ACTB and ALB) are abundant proteins with a degree of connectivity that is somewhat indicative of network topology and not necessarily of the disease-specificity and were therefore taken with caution.

This picture is confirmed by the enrichment analysis of the hub genes. It pointed to transcriptional regulation, nuclear receptor and hormone-related functions, SMAD binding and T-helper 17 (Th17) cell lineage commitment, while the KEGG analysis highlighted the type 1 diabetes and inflammatory bowel disease pathways. These terms are best interpreted as indicators of common immune and cytokine signalling, mainly mediated by TNF, IL6, IL1B, STAT3 and INS. They are not evidence per se for the effect of the metabolites on type 1 diabetes or inflammatory bowel disease. Their applicability to T2DM, however, is still reasonable. Th17 cells have been linked to obesity, insulin resistance and inflammatory bowel disease (Zi *et al.,* 2022), and immune–metabolic cross-talk is now considered part of T2DM pathogenesis (Rohm *et al.,* 2022). The SMAD binding pathway to TGF-β/SMAD signalling controls inflammatory and fibrotic pathways relevant to diabetic complications, and the nuclear receptor pathway is of interest as nuclear receptors like PPAR-γ are known targets for antidiabetic drugs. Taken together, the enrichment profile suggests that the predicted effects of the fruit metabolites converge on inflammatory and transcriptional regulation of insulin action. This is the context in which the two docking targets were chosen.

AKT1 and GAPDH were chosen as the two complementary arms of the disease. AKT1 (also known as protein kinase B) is one of the major kinases of the PI3K–AKT pathway that helps insulin to promote glucose uptake and glycogenesis; insulin resistance is characterized by a number of abnormalities in this pathway (Huang *et al.,* 2018). The AKT1 gene has also been linked to the pathogenesis of T2DM and its complications (Kochetova *et al.,* 2024). GAPDH is a glycolytic enzyme whose inhibition under hyperglycaemia diverts glycolytic intermediates towards the polyol, advanced glycation and protein kinase C routes of diabetic damage (Brownlee, 2005). Targeting these two proteins may therefore address insulin impairment and hyperglycaemia-driven complications at the same time, and both sit among the top-ranked hubs.

The network results are backed by the docking results. The co-crystallised AKT1 ligand scored −9.4 kcal/mol and the GAPDH reference −7.0 kcal/mol. Against AKT1, twenty metabolites scored better than the reference, led by C513 (−11.9), C151 (−11.4), C20 (−11.0), C928 (−10.9) and C427 (−10.6). Against GAPDH, eighty-one metabolites scored better than the reference, led by C1403 (−9.7), C20 (−9.4), C25 (−9.4), C513 (−9.3) and C1382 (−9.2). Twenty metabolites exceeded both references, and C20 and C513 were in the top group for both proteins, indicating dual-target potential, whereas C1382 and C1403 showed good activity against GAPDH only. The network view would expect the most valuable compound to be a dual-target compound, as this supports the multi-target rationale much better than a single-target binder. C20 is a p-coumaroylquinic acid derivative, and C34, which also scored better than the AKT1 reference (−10.4), is a dicinnamoylquinic acid. Both are members of the chlorogenic acid family, which has been reported to have several antidiabetic effects, including the ability to bind the pleckstrin homology domain of AKT, thereby promoting its phosphorylation (Gao *et al.,* 2018), and the potential to inhibit starch-digesting enzymes (Adisakwattana, 2017; Yu *et al.,* 2024). Other high-scoring metabolites, notably C25, C151, C513 and C1403, were annotated as an aromatic amide, a cephalosporin-type compound, an aliphatic diester and a cyclopropane-containing fatty acid. The occurrence of these classes in plant extracts is rare, and their structure needs to be verified by MS/MS matching, authentic standard, or natural product databases prior to any subsequent studies.

These scores are explained at the residue level by the interaction patterns. In AKT1, all five best metabolites contacted LYS179, VAL164 and LEU156, as did the reference ligand, and these residues line the ATP-binding pocket (Jamshidi *et al.,* 2025). C25 also formed a hydrogen bond with the hinge residue ALA230, which is listed among the critical residues of the Akt1 ATP-binding site (Jamshidi *et al.,* 2025). Hinge contacts are typical of ATP-competitive kinase inhibitors, which suggests that the metabolites occupy the same site as the reference and not an unrelated surface. In GAPDH, the hydrogen bonding between C513 and C1382 and between CYS152 and both of them was observed, as well as the contact between C25 and CYS152. CYS152 is the active-site cysteine that attacks glyceraldehyde 3-phosphate during catalysis (Canarelli *et al.,* 2022), and C25, C513 and C1382 also contacted HIS179, as did the reference. Contacts in the catalytic region therefore suggest that these ligands compete for the substrate site. Sharing contacts with the reference ligands makes the predicted binding modes more plausible, but docking scores rank compounds by predicted affinity and are best read as a tool for prioritising candidates (Paggi *et al.,* 2024).

These observations are in accord with the general literature. Other antidiabetic plants showed that phenolic and flavonoid compounds had high connectivity scores in network pharmacology studies against the hub targets, including AKT1 (Jiao *et al.,* 2021; Ononamadu & Seidel, 2024; Ononamadu *et al.,* 2025; Zubair *et al.,* 2025). In a docking study of the AKT1 ATP site, flavonoid glycosides, including kaempferol glycosides, rutin, isoquercitrin and cynaroside, scored better than the reference inhibitor ipatasertib (Jamshidi *et al.,* 2025). This is consistent in direction with our result that the natural can outscore the AKT1 with a different absolute value since it was done with AutoDock 4 and a different scoring function. The result of the GAPDH is also of interest, from an immunological point of view. Inhibiting GAPDH with the covalent inhibitor koningic acid lowered the production of TNF-α, IFN-γ and IL-2 by activated Th1 cells (Canarelli *et al.,* 2022), which links this glycolytic hub to the same inflammatory network highlighted by the enrichment analysis. The effect of GAPDH modulation is therefore context dependent, as it could be used to dampen the production of immune cytokines, but hyperglycaemia-driven inhibition of GAPDH is a source of vascular and tissue damage (Brownlee, 2005).

The caveat brings the main implications of this work. Firstly, the results provide a molecular explanation for the traditional application of the fruit in diabetes, as the predicted targets are related to insulin signalling, glycolytic stress and inflammation, consistent with the multi-target approach of antidiabetic plants (Panossian, 2025). Second, they provide a short list for experimental testing, namely C513, C151 and C20 for AKT1 and C1403, C20 and C25 for GAPDH, with C20 and C513 ranking highly for both targets. The testing of these in AKT1 and GAPDH activity assays, and in insulin-resistant cell models, is a much more efficient process than screening the entire library. Third, the chlorogenic acid-type hits (C20 and C34) are the most chemically familiar and the most likely to be obtainable as standards. Fourth, binding does not reveal functional direction. An ATP site inhibitor of

AKT would be predicted to inhibit the kinase activity of AKT1 and insulin sensitisation would need to be mediated by increased or normal AKT activity, with the same level of uncertainty being applied to GAPDH. These metabolites will be either inhibitors, activators or modulators and whether combined across the network they are different from the single target effects can only be answered by experiments.

As with all computational predictions, these findings are hypotheses that need experimental testing. Network pharmacology depends on the degree of coverage of the databases and docking scores are only approximations of the binding affinity. Some annotations are putative, so the identity of key metabolites will need to be confirmed with standards. Future studies will therefore isolate or obtain standards of the most highly-ranked metabolites and subject them to AKT1 and GAPDH activity assays, as well as insulin-resistant cell models, and will analyze the stability of the most active complexes by molecular dynamics and binding free energy calculations. The most promising metabolites can then be tested in animal models of diabetes, with toxicity also screened.

5.0 Conclusion

This study used network pharmacology and molecular docking to predict how metabolites previously identified from *Gongronema latifolium* fruit may act against type 2 diabetes mellitus. Predicted targets are in line with a multi-target approach: insulin signalling, glycolytic stress and inflammation. The primary predicted targets were AKT1 and GAPDH and a limited subset of metabolites yielded binding scores that were better than those of the co-crystallised reference ligands. These are computational predictions and should be interpreted as hypotheses; they suggest how to treat the traditional use of the fruit, but offer no proof of the treatment. Essential next steps are confirmation of metabolite identity, enzyme assays, cell-based insulin-signalling tests and molecular dynamics, followed by safety and toxicity assessment and *in vivo* studies.

REFERENCES

Accili, D., Deng, Z., & Liu, Q. (2025). Insulin resistance in type 2 diabetes mellitus. Nature Reviews Endocrinology, 21, 413–426. https://doi.org/10.1038/s41574-025-01114-y

Adisakwattana, S. (2017). Cinnamic acid and its derivatives: Mechanisms for prevention and management of diabetes and its complications. Nutrients, 9(2), 163.

Amberger, J. S., Bocchini, C. A., Scott, A. F., & Hamosh, A. (2019). OMIM.org: Leveraging knowledge across phenotype–gene relationships. Nucleic Acids Research, 47(D1), D1038–D1043. https://doi.org/10.1093/nar/gky1151

Amrelia. (2022). Nutritive and medicinal value of Gongronema latifolium. Journal of Natural Products Discovery, 1(2). https://doi.org/10.24377/jnpd.article751

Berman, H. M., Westbrook, J., Feng, Z., Gilliland, G., Bhat, T. N., Weissig, H., Shindyalov, I. N., & Bourne, P. E. (2000). The Protein Data Bank. Nucleic Acids Research, 28(1), 235–242. https://doi.org/10.1093/nar/28.1.235

Beshel, J. A., Palacios, J., Beshel, F. N., Nku, C. O., Owu, D. U., Nwokocha, M., Bórquez, J., Simirgiotis, M. J., & Nwokocha, C. R. (2025). In silico molecular docking study and antihypertensive property of Gongronema latifolium Benth. ethanol leaf extract in dexamethasone-induced hypertension in Wistar rats. Phytomedicine Plus, 5(4), 100892. https://doi.org/10.1016/j.phyplu.2025.100892

Brownlee, M. (2005). The pathobiology of diabetic complications: A unifying mechanism. Diabetes, 54(6), 1615–1625.

Canarelli, S. E., Swalm, B. M., Larson, E. T., Morrison, M. J., & Weerapana, E. (2022). Monitoring GAPDH activity and inhibition with cysteine-reactive chemical probes. RSC Chemical Biology, 3(7), 972–982. https://doi.org/10.1039/d2cb00091a

Chin, C.-H., Chen, S.-H., Wu, H.-H., Ho, C.-W., Ko, M.-T., & Lin, C.-Y. (2014). cytoHubba: Identifying hub objects and sub-networks from complex interactome. BMC Systems Biology, 8(Suppl 4), S11. https://doi.org/10.1186/1752-0509-8-S4-S11

Daina, A., Michielin, O., & Zoete, V. (2017). SwissADME: A free web tool to evaluate pharmacokinetics, drug-likeness and medicinal chemistry friendliness of small molecules. Scientific Reports, 7, 42717. https://doi.org/10.1038/srep42717

Daina, A., Michielin, O., & Zoete, V. (2019). SwissTargetPrediction: Updated data and new features for efficient prediction of protein targets of small molecules. Nucleic Acids Research, 47(W1), W357–W364. https://doi.org/10.1093/nar/gkz382

Dallakyan, S., & Olson, A. J. (2015). Small-molecule library screening by docking with PyRx. Methods in Molecular Biology, 1263, 243–250. https://doi.org/10.1007/978-1-4939-2269-7_19

Donath, M. Y., & Shoelson, S. E. (2011). Type 2 diabetes as an inflammatory disease. Nature Reviews Immunology, 11(2), 98–107.

Gao, J., He, X., Ma, Y., Zhao, X., Hou, X., Hao, E., Deng, J., & Bai, G. (2018). Chlorogenic acid targeting of the AKT PH domain activates AKT/GSK3β/FOXO1 signaling and improves glucose metabolism. Nutrients, 10(10), 1366. https://doi.org/10.3390/nu10101366

Ge, S. X., Jung, D., & Yao, R. (2020). ShinyGO: A graphical gene-set enrichment tool for animals and plants. Bioinformatics, 36(8), 2628–2629. https://doi.org/10.1093/bioinformatics/btz931

Genitsaridi, I., Salpea, P., Salim, A., Sajjadi, S. F., Tomic, D., James, S., … (2026). 11th edition of the IDF Diabetes Atlas: Global, regional, and national diabetes prevalence estimates for 2024 and projections for 2050. The Lancet Diabetes & Endocrinology, 14, 149–156. https://doi.org/10.1016/s2213-8587(25)00299-2

Gyebi, G. A., Afolabi, S. O., Ogunyemi, O. M., Ibrahim, I. M., Olorundare, O. E., Adebayo, J. O., & Koketsu, M. (2024). Apoptotic potential of iloneoside from Gongronema latifolium Benth against prostate cancer cells using in vitro and in silico approach. Cell Biochemistry and Biophysics. https://doi.org/10.1007/s12013-024-01507-2

Huang, X., Liu, G., Guo, J., & Su, Z. (2018). The PI3K/AKT pathway in obesity and type 2 diabetes. International Journal

of Biological Sciences, 14(11), 1483–1496. https://doi.org/10.7150/ijbs.27173

Jamshidi, S., Eghbalian, A., Shojaei, S., Taherkhani, A., & Feizi-Dehnayebi, M. (2025). Flavonoids as promising Akt1 inhibitors in cancer medicine: Insights from molecular docking, dynamics, DFT calculations, and in vitro validation. Cancer Reports, 8(8), e70315. https://doi.org/10.1002/cnr2.70315

Jiao, X., Jin, X., Ma, Y., Yang, Y., Li, J., Liang, L., Liu, R., & Li, Z. (2021). A comprehensive application: Molecular docking and network pharmacology for the prediction of bioactive constituents and elucidation of mechanisms of action in component-based Chinese medicine. Computational Biology and Chemistry, 90, 107402.

Kim, S., Chen, J., Cheng, T., Gindulyte, A., He, J., He, S., Li, Q., Shoemaker, B. A., Thiessen, P. A., Yu, B., Zaslavsky, L., Zhang, J., & Bolton, E. E. (2025). PubChem 2025 update. Nucleic Acids Research, 53(D1), D1516–D1525. https://doi.org/10.1093/nar/gkae1059

Kochetova, O. V., Shangareeva, Z. A., Avsaleydiniva, D. S., Viktorova, T. V., & Korytina, G. F. (2024). The role of the AKT1 gene in the pathogenesis of type 2 diabetes mellitus and its complications. Molekulyarnaya Meditsina, 22(3), 57–64.

Lipinski, C. A., Lombardo, F., Dominy, B. W., & Feeney, P. J. (2001). Experimental and computational approaches to estimate solubility and permeability in drug discovery and development settings. Advanced Drug Delivery Reviews, 46(1–3), 3–26. https://doi.org/10.1016/s0169-409x(00)00129-0

Mahmoud, V. L., Shayesteh, R., Loh, T. K. F. Y., Chan, S. W., Sethi, G., Burgess, K., Lee, S. H., Wong, W. F., & Looi, C. Y. (2024). Comprehensive review of opportunities and challenges of ethnomedicinal plants for managing type 2 diabetes. Heliyon, 10, e39699. https://doi.org/10.1016/j.heliyon.2024.e39699

Młynarska, E., Czarnik, W., Dzieża, N., Jędraszak, W., Majchrowicz, G., Prusinowski, F., Stabrawa, M., Rysz, J., & Franczyk, B. (2025). Type 2 diabetes mellitus: New pathogenetic mechanisms, treatment and the most important complications. International Journal of Molecular Sciences, 26(3), Article 1094. https://doi.org/10.3390/ijms26031094

O'Boyle, N. M., Banck, M., James, C. A., Morley, C., Vandermeersch, T., & Hutchison, G. R. (2011). Open Babel: An open chemical toolbox. Journal of Cheminformatics, 3, 33. https://doi.org/10.1186/1758-2946-3-33

Ogunyemi, O. M., Gyebi, G. A., Saheed, A., Paul, J., Nwaneri-Chidozie, V., Olorundare, O., … (2022). Inhibition mechanism of alpha-amylase, a diabetes target, by a steroidal pregnane and pregnane glycosides derived from Gongronema latifolium Benth. Frontiers in Molecular Biosciences, 9, 866719. https://doi.org/10.3389/fmolb.2022.866719

Ojo, O. A., Gyebi, G. A., Iyobhebhe, M., Dada, S., Daramola, T., Ojo, A. B., … (2026). Deciphering the mechanisms underlying the dual-target inhibition of carbohydrate-digesting and neurodegenerative enzymes by Syzygium aromaticum (L.) Merr. & L.M. via molecular docking and dynamics simulations. Scientific Reports, 16. https://doi.org/10.1038/s41598-026-45482-5

Ojo, O. A., Ogunlakin, A. D., Ajayi-Odoko, O. A., Gyebi, G. A., Ayokunle, D. I., Olanrewaju, A. A., … (2025). Bioprospection of indigenous herbal formulations for diabetes care: In vitro, network pharmacology, and molecular dynamics studies. BMC Complementary Medicine and Therapies, 25, 225. https://doi.org/10.1186/s12906-025-04980-1

Okochi, C., Asogwa, K., Ezenwelu, C., Nwolisah, O., & Ehichanya, C. (2024). Comparative proximate, phytochemical composition and antioxidant activity on aqueous extract of Gongronema latifolium fruit and leaf. The Bioscientist, 12.

Ononamadu, C. J., & Seidel, V. (2024). Exploring the antidiabetic potential of Salvia officinalis using network pharmacology, molecular docking and ADME/drug-likeness predictions. Plants, 13(20), Article 2892. https://doi.org/10.3390/plants13202892

Ononamadu, C. J., Ben Ahmed, Z., & Seidel, V. (2025). Network pharmacology, molecular docking and molecular dynamics studies to predict the molecular targets and mechanisms of action of Melissa officinalis phytoconstituents in type-2 diabetes mellitus. Plants, 14(18), Article 2828. https://doi.org/10.3390/plants14182828

Paggi, J. M., Pandit, A., & Dror, R. O. (2024). The art and science of molecular docking. Annual Review of Biochemistry, 93. https://doi.org/10.1146/annurev-biochem-030222-120000

Panossian, A. (2025). Trends and pitfalls in the progress of network pharmacology research on natural products. Pharmaceuticals, 18(4), Article 538. https://doi.org/10.3390/ph18040538

Piñero, J., Ramírez-Anguita, J. M., Saüch-Pitarch, J., Ronzano, F., Centeno, E., Sanz, F., … (2020). The DisGeNET knowledge platform for disease genomics: 2019 update. Nucleic Acids Research, 48(D1), D845–D855. https://doi.org/10.1093/nar/gkz1021

Rappaport, N., Twik, M., Plaschkes, I., Nudel, R., Iny Stein, T., Levitt, J., … (2017). MalaCards: An amalgamated human disease compendium with diverse clinical and genetic annotation and structured search. Nucleic Acids Research, 45(D1), D877–D887. https://doi.org/10.1093/nar/gkw1012

Rappé, A. K., Casewit, C. J., Colwell, K. S., Goddard, W. A., III, & Skiff, W. M. (1992). UFF, a full periodic table force field for molecular mechanics and molecular dynamics simulations. Journal of the American Chemical Society, 114(25), 10024–10035. https://doi.org/10.1021/ja00051a040
Rohm, T. V., Meier, D. T., Olefsky, J. M., & Donath, M. Y. (2022). Inflammation in obesity, diabetes, and related disorders. Immunity, 55(1), 31–55. https://doi.org/10.1016/j.immuni.2021.12.013

Shannon, P., Markiel, A., Ozier, O., Baliga, N. S., Wang, J. T., Ramage, D., … (2003). Cytoscape: A software environment for integrated models of biomolecular interaction networks. Genome Research, 13(11), 2498–2504. https://doi.org/10.1101/gr.1239303

Szklarczyk, D., Nastou, K., Koutrouli, M., Kirsch, R., Mehryary, F., Hachilif, R., Hu, D., Peluso, M. E., Huang, Q., Fang, T., Doncheva, N. T., Pyysalo, S., Bork, P., Jensen, L. J., & von Mering, C. (2025). The STRING database in 2025: Protein networks with directionality of regulation. Nucleic Acids Research, 53(D1), D730–D737. https://doi.org/10.1093/nar/gkae1113

Trott, O., & Olson, A. J. (2010). AutoDock Vina: Improving the speed and accuracy of docking with a new scoring function, efficient optimization, and multithreading. Journal of Computational Chemistry, 31(2), 455–461. https://doi.org/10.1002/jcc.21334

Wang, X., Shen, Y., Wang, S., Li, S., Zhang, W., Liu, X., … (2017). PharmMapper 2017 update: A web server for potential drug target identification with a comprehensive target pharmacophore database. Nucleic Acids Research, 45(W1), W356–W360. https://doi.org/10.1093/nar/gkx374

Yu, M., Zhu, S., Huang, D., Tao, X., & Li, Y. (2024). Inhibition of starch digestion by phenolic acids with a cinnamic acid backbone: Structural requirements for the inhibition of α-amylase and α-glucosidase. Food Chemistry, 435, 137499.

Zi, C., Wang, D., Gao, Y., & He, L. (2022). The role of Th17 cells in endocrine organs: Involvement of the gut, adipose tissue, liver and bone. Frontiers in Immunology, 13, 1104943. https://doi.org/10.3389/fimmu.2022.1104943

Zubair, M. S., Yuyun, Y., Musnina, W. S., Najib, A., Nainu, F., Arba, M., Paneo, D. R., Praditapuspa, E. N., & Maulana, S. (2025). Network pharmacology and molecular docking studies of ethnopharmacological plants from Sulawesi as antidiabetics. Tropical Journal of Natural Product Research, 9(3). https://doi.org/10.26538/tjnpr/v9i3.30

©2026 This is an Open Access article distributed under the terms of the Creative Commons Attribution 4.0 International license viewed via https://creativecommons.org/licenses/by/4.0/ which permits unrestricted use, distribution, and reproduction in any medium, provided the original work is cited appropriately.